

De Novo and Inherited Pathogenic Variants in *KDM3B* Cause Intellectual Disability, Short Stature, and Facial Dysmorphism

Illja J. Diets,¹ Roos van der Donk,^{1,2} Kristina Baltrunaite,³ Esmé Waanders,² Margot R.F. Reijnders,^{1,4} Alexander J.M. Dingemans,¹ Rolph Pfundt,¹ Anneke T. Vulto-van Silfhout,¹ Laurens Wiel,^{1,5} Christian Gilissen,^{1,5} Julien Thevenon,^{6,7} Laurence Perrin,⁶ Alexandra Afenjar,⁸ Caroline Nava,^{9,10} Boris Keren,⁹ Sarah Bartz,¹¹ Bethany Peri,¹¹ Gea Beunders,¹² Nienke Verbeek,¹³ Koen van Gassen,¹³ Isabelle Thiffault,^{14,15,16} Maxime Cadieux-Dion,^{14,15} Lina Huerta-Saenz,^{17,18} Matias Wagner,^{19,20,21} Vassiliki Konstantopoulou,²² Julia Vodopituz,²² Matthias Griese,²³ Annekatrien Boel,²⁴ Bert Callewaert,²⁴ Han G. Brunner,^{1,25,26} Tjitske Kleefstra,^{1,25} Nicoline Hoogerbrugge,¹ Bert B.A. de Vries,¹ Vivian Hwa,³ Andrew Dauber,^{3,27} Jayne Y. Hehir-Kwa,² Roland P. Kuiper,^{1,2} and Marjolijn C.J. Jongmans^{1,2,13,*}

By using exome sequencing and a gene matching approach, we identified *de novo* and inherited pathogenic variants in *KDM3B* in 14 unrelated individuals and three affected parents with varying degrees of intellectual disability (ID) or developmental delay (DD) and short stature. The individuals share additional phenotypic features that include feeding difficulties in infancy, joint hypermobility, and characteristic facial features such as a wide mouth, a pointed chin, long ears, and a low columella. Notably, two individuals developed cancer, acute myeloid leukemia and Hodgkin lymphoma, in childhood. *KDM3B* encodes for a histone demethylase and is involved in H3K9 demethylation, a crucial part of chromatin modification required for transcriptional regulation. We identified missense and truncating variants, suggesting that *KDM3B* haploinsufficiency is the underlying mechanism for this syndrome. By using a hybrid facial-recognition model, we show that individuals with a pathogenic variant in *KDM3B* have a facial gestalt, and that they show significant facial similarity compared to control individuals with ID. In conclusion, pathogenic variants in *KDM3B* cause a syndrome characterized by ID, short stature, and facial dysmorphism.

Intellectual disability (ID) and autism spectrum disorder are neurodevelopmental disorders (NDDs) that occur in approximately 1%–3% of the general population.^{1,2} The introduction of next-generation sequencing techniques as a diagnostic test for individuals with unexplained NDD has led to the discovery of many disease-causing mutations in genes previously unassociated with disease.^{3–6} However, a subset of individuals remain without a diagnosis. By using trio-based exome sequencing in diagnostic or research settings as described before,^{5,7–10} and by collaborating via GeneMatcher,¹¹ we identified

17 individuals with heterozygous missense and truncating variants in *KDM3B* (lysine-specific demethylase 3B [MIM: 609373; GenBank: NM_016604.3]; Figure 1A). All 14 different variants found were absent from the gnomAD and ExAC databases, and 13/14 had high Combined Annotation Dependent Depletion scores (CADD; scores between 13 and 40) and were predicted to be pathogenic by both the PolyPhen-2 and SIFT prediction programs (Table 1).^{12–15} All individuals or their legal guardians gave written informed consent, and the study was given IRB approval.

¹Department of Human Genetics, Radboud University Medical Center, 6525GA Nijmegen, the Netherlands; ²Princess Máxima Center for Pediatric Oncology, 3584CS Utrecht, the Netherlands; ³Division of Endocrinology, Cincinnati Center for Growth Disorders, Cincinnati Children's Hospital Medical Center, Department of Pediatrics, University of Cincinnati College of Medicine, Cincinnati, OH 45229, USA; ⁴Department of Clinical Genetics, Maastricht University Medical Center, 6229HX Maastricht, the Netherlands; ⁵Centre for Molecular and Biomolecular Informatics, Radboud Institute for Molecular Life Sciences, Radboud University Medical Center, 6525GA Nijmegen, the Netherlands; ⁶Centre de Génétique et Centre de Référence Anomalies du Développement et Syndromes Malformatifs, Hôpital d'Enfants, Centre Hospitalier Universitaire de Dijon, 21079 Dijon, France; ⁷Equipe Génétique des Anomalies du Développement, Université de Bourgogne-France Comté, 21070 Dijon, France; ⁸APHP, Département de Génétique et Embryologie Médicale, Centre de Référence Déficiences Intellectuelles de Causes Rares, GRC n°19, ConCer-LD, Hôpital Armand Trousseau, 75012 Paris, France; ⁹APHP, Hôpital Pitié-Salpêtrière, Département de Génétique, 75013, Paris, France; ¹⁰Sorbonne Universités, Institut du Cerveau et de la Moelle épinière, ICM, Institut National de la Santé et de la Recherche Médicale U1127, Centre National de la Recherche Scientifique UMR 7225, 75013, Paris, France; ¹¹Division of Endocrinology, Children's Hospital of Colorado, Aurora, CO 80045, USA; ¹²Department of Clinical Genetics, VU University Medical Center, 1081HV Amsterdam, the Netherlands; ¹³Department of Genetics, University Medical Center Utrecht, 3508AB Utrecht, the Netherlands; ¹⁴Center for Pediatric Genomic Medicine, Children's Mercy Hospital, Kansas City, MO 66211, USA; ¹⁵Department of Pathology and Laboratory Medicine, Children's Mercy Hospital, Kansas City, MO 66211, USA; ¹⁶University of Missouri, Kansas City School of Medicine, Kansas City, MO 66211, USA; ¹⁷Children's Mercy Hospital, Kansas City, MO 66211, USA; ¹⁸Division of Pediatric Endocrinology and Diabetes, Department of Pediatrics, Penn State Hershey Children's Hospital, Hershey, PA 17033, USA; ¹⁹Institute of Human Genetics, Technische Universität München, 80333 Munich, Germany; ²⁰Institute for Neurogenetics, Helmholtz Zentrum München, 85764 Neuherberg, Germany; ²¹Institute for Human Genetics, Helmholtz Zentrum München, 85764 Neuherberg, Germany; ²²Department of Pediatrics and Adolescent Medicine, Medical University of Vienna, 1090 Vienna, Austria; ²³Dr. von Hauner Children's Hospital, Division of Pediatric Pneumology, University Hospital Munich, German Center for Lung Research, 80333 Munich, Germany; ²⁴Center for Medical Genetics, Ghent University Hospital, 9000 Ghent, Belgium; ²⁵Donders Institute for Brain, Cognition and Behavior, Radboud University Nijmegen, 6525GA Nijmegen, the Netherlands; ²⁶Department of Clinical Genetics and School for Oncology & Developmental Biology (GROW), Maastricht University Medical Center, 6202AZ Maastricht, the Netherlands; ²⁷Division of Endocrinology, Children's National Health System, Washington, DC 20010, USA

*Correspondence: m.c.j.jongmans-3@umcutrecht.nl

<https://doi.org/10.1016/j.ajhg.2019.02.023>

© 2019 American Society of Human Genetics.



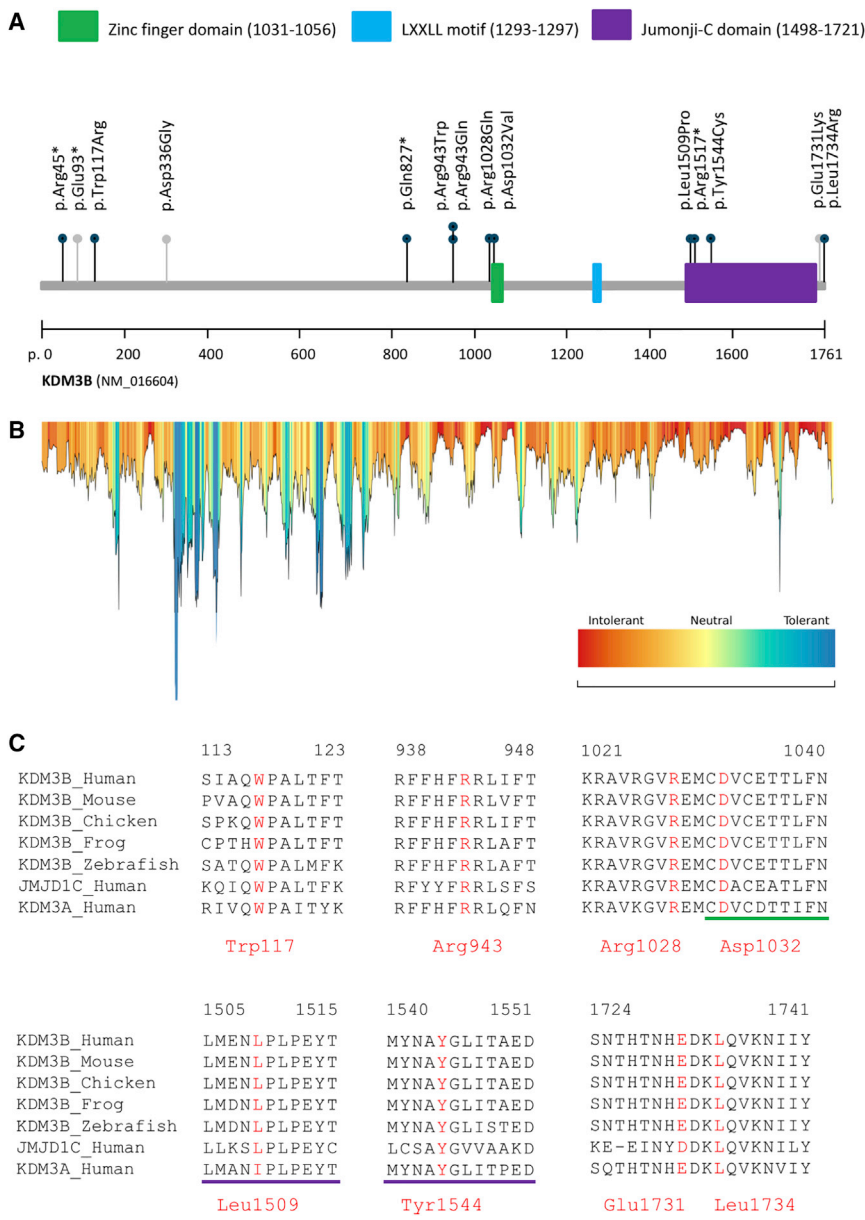


Figure 1. *KDM3B* Germline Variants and Amino Acid Sequence Conservation

(A) A schematic representation of *KDM3B*, including the zinc-finger domain, LXXLL motif, and Jumonji-C domain, showing the location of the reported variants according to their position at the protein level. The gray lollipop represents the variants that were inherited from similarly affected parents. As indicated, truncating variants were identified in five individuals and missense variants in 12 individuals.

(B) A tolerance landscape plot provided by the MetaDome web server for the analysis of *KDM3B*. For quantifying genetic tolerance, a missense-over-synonymous ratio based on the variations reported in the gnomAD database is calculated. This ratio is computed into a tolerance landscape as a sliding window of 11 residues over the protein.³⁰ For *KDM3B*, this plot shows intolerance for missense variation in and nearby the zinc-finger and Jumonji-C domains, where most of the missense mutations identified in the individuals described in this paper are located.

(C) Protein alignment of *KDM3B* orthologs across several species. Additionally, we aligned JMJD1C and *KDM3A*. These proteins show homology with *KDM3B* and share the same functional domains. As shown, the Trp117, Arg943, Arg1028, Asp1032, Leu1509, Tyr1544, Glu1731, and Leu1734 positions (shown in red) are evolutionarily highly conserved.

In ten individuals, the variants identified were confirmed to be *de novo*, and in three other individuals (individuals 1, 6, and 16) the variants were inherited from similarly affected parents (individuals 2, 7, and 17), summing up to 16 individuals. In one additional individual with a protein-truncating variant (individual 14), no paternal DNA was available for segregation analysis, but we confirmed that the variant was not maternally inherited. Phenotypic data for the individuals is shown in Table 2 and Table S1. The 17 individuals (9 females and 8 males) were all diagnosed with developmental delay (DD) or mild to moderate ID, although one individual (individual 14) was too young for development to be assessed. The individuals show both delayed motor and delayed speech developments, although the language delays are more pronounced. Behavior problems were noted in eight individuals: there was a diagnosis of attention deficit hyperactivity disorder (ADHD) in four

individuals and a diagnosis of autism spectrum disorder in three individuals. Notably, two individuals had a double diagnosis of autism spectrum disorder combined with ADHD. Three other individuals showed aggressive behavior, hyperactivity, and delayed social-emotional development, but they did not have formal psychiatric diagnoses. Other neurological problems included epilepsy in three individuals and childhood hypotonia in five individuals. In two out of three individuals with epilepsy, the epilepsy showed a transient character.

Eight individuals presented with short stature, defined as a height below -2.5 SD. Microcephaly was reported in one individual, whereas the others had normal head circumferences. Other recurrent features included neonatal feeding difficulties ($n = 9$), eye abnormalities ($n = 5$), hearing loss ($n = 4$), joint hypermobility ($n = 5$), and hematological malignancies ($n = 2$). The eye abnormalities consisted of ocular movement disorders such as nystagmus and strabismus in four individuals and refraction anomalies and low vision in three individuals. Furthermore, the individuals displayed a wide range of congenital anomalies, including umbilical and inguinal hernias, cryptorchidism, hypospadias, ventricular septal defect, interrupted inferior

Table 1. In Silico Analysis of KDM3B Variants Identified

Ind.	mRNA Change	Predicted Protein Effect	Inheritance	gnomAD	PhyloP	CADD Score	PolyPhen-2	SIFT	MetaDome Tolerance ^a
1	c.133C>T	p.Arg45*	de novo	0	4.08	38	NA	NA	NA
2	c.277G>T	p.Glu93*	maternal	0	4.00	35	NA	NA	NA
3 ^b	c.277G>T	p.Glu93*	ND	0	4.00	35	NA	NA	NA
4	c.349T>C	p.Trp117Arg	de novo	0	3.35	20.2	probably damaging	deleterious	neutral
5	c.1007A>G	p.Asp336Gly	maternal	0	2.06	13.8	benign	deleterious	tolerant
6 ^b	c.1007A>G	p.Asp336Gly	ND	0	2.06	13.8	benign	deleterious	tolerant
7	c.2479C>T	p.Gln827*	ND	0	2.79	33	NA	NA	NA
8	c.2827C>T	p.Arg943Trp	de novo	0	4.32	25.9	probably damaging	deleterious	intolerant
9	c.2828G>A	p.Arg943Gln	de novo	0	6.34	36	probably damaging	deleterious	intolerant
10	c.3083G>A	p.Arg1028Gln	de novo	0	6.18	37	probably damaging	deleterious	highly intolerant
11	c.3095A>T	p.Asp1032Val	de novo	0	4.97	32	probably damaging	deleterious	highly intolerant
12	c.4526T>C	p.Leu1509Pro	de novo	0	4.81	23.2	probably damaging	deleterious	intolerant
13	c.4549C>T	p.Arg1517*	de novo	0	2.55	40	NA	NA	NA
14	c.4631A>G	p.Tyr1544Cys	de novo	0	4.97	23	probably damaging	deleterious	highly intolerant
15	c.5191G>A	p.Glu1731Lys	paternal	0	6.26	23.5	probably damaging	deleterious	intolerant
16 ^b	c.5191G>A	p.Glu1731Lys	ND	0	6.26	23.5	probably damaging	deleterious	intolerant
17	c.5201T>G	p.Leu1734Arg	de novo	0	5.13	18	probably damaging	deleterious	intolerant

Abbreviations are as follows: Ind. = individual; CADD = Combined Annotation Dependent Depletion; SIFT = Sorting Intolerant From Tolerant; ND = not determined; and NA = not applicable.

^aThe MetaDome tolerance is based on the tolerance colors of the web server MetaDome.³⁰

^bIndividuals 3, 6, and 16 are the mother, father, and mother of individuals 2, 5, and 15, respectively.

vena cava, diaphragmatic hernia, heterotaxy, duodenal atresia, pulmonary capillary hemangiomatosis, and congenital hip dysplasia. With the exception of the umbilical hernia, the inguinal hernia, and the diaphragmatic hernia (all three present in two individuals), none of the congenital anomalies were recurrent in multiple individuals. No clear genotype-phenotype correlation could be observed. Shared facial characteristics in the majority of the individuals were long ears ($n = 9$), a broad nasal tip ($n = 14$), a low-hanging columella ($n = 6$), a wide mouth ($n = 12$), a thin upper lip vermillion ($n = 12$), and a pointed chin ($n = 12$), as shown in [Figure 2](#).

On the basis of these shared dysmorphic features, we hypothesized that facial recognition software would be able to detect common facial features in individuals with missense and truncating variants in *KDM3B*. Facial recognition software is able to objectively detect subtle features which might be difficult to identify by eye.^{16–18} In the past, facial recognition software has been used to objectively measure dysmorphic features in individuals with various syndromes.^{17–19} We collected and analyzed photographs of 13 out of 14 children. The three affected parents were deliberately excluded to avoid a bias caused by facial features that were shared with their children and unrelated to the variant identified. To determine whether a facial gestalt is present in individuals with a variant in *KDM3B*, we used a hybrid model recently developed and described

by van der Donk et al.²⁰ This hybrid model combines the output of two computer vision algorithms: Clinical Face Phenotype Space (CFPS)²¹ and OpenFace.²² In this hybrid method, the resulting two output feature vectors from these algorithms are combined, giving a 468-dimensional hybrid feature vector that represents the facial features of an individual. Because the CFPS and OpenFace algorithms were trained to recognize dysmorphic features and general facial features, respectively, both algorithms recognize different facial characteristics, and the combined hybrid model uses both of these different feature types to improve the distinction between subtle differences in these dysmorphic features (details in van der Donk et al.²⁰).

To determine the similarity between individuals with a variant in *KDM3B* versus a control population consisting of 130 individuals with other ID-syndromes, we calculated the clustering improvement factors (CIFs), which give an estimate of search space reduction.²¹ In brief, the CIF estimates how a group of affected individuals cluster within a group of controls and compares that clustering to what is expected by random chance. For each individual, ten ID-affected controls that were matched for age, gender, and ethnicity were selected. We used ID-affected controls instead of healthy control individuals so that we could determine whether we are able to distinguish individuals with a variant in *KDM3B* from the general ID-affected population.

Table 2. Clinical Characteristics of Individuals with *KDM3B* Variants

	Percentage	Number
Development		
Intellectual disability or developmental delay	94.1%	16/17 ^a
Developmental delay	23.5%	4/17
Mild disability	47.1%	8/17
Mild to moderate or moderate disability	23.5%	4/17
Growth		
Short stature (<-2.5 SD)	50.0%	8/16
Height <-1.5 SD	68.8%	11/16
Neurological		
Behavior problems	53.3%	8/15 ^b
ADHD	26.7%	4/15
Autism spectrum disorder	20.0%	3/15
Other	13.3%	2/15
Epilepsy	20.0%	3/15
Childhood hypotonia	38.5%	5/13
Congenital Anomalies		
Umbilical hernia	12.5%	2/16
Inguinal hernia	12.5%	2/16
Cryptorchidism	12.5%	1/8
Hypospadias	12.5%	1/8
Congenital hip dysplasia	6.3%	1/16
Congenital hypothyroidism	6.3%	1/16
Diaphragmatic hernia	12.5%	2/16
Heterotaxy	6.3%	1/16
Interrupted inferior vena cava	6.3%	1/16
Duodenal atresia	6.3%	1/16
Other		
Neonatal feeding difficulties	60%	9/15
Joint hypermobility	31.3%	5/16
Eye abnormalities	31.3%	5/16
Hearing loss	23.5%	4/17
Malignancy	11.8%	2/17

Abbreviations are as follows: ADHD = attention deficit hyperactivity disorder.

^aIndividual 14 is still too young to determine her development.

^bTwo individuals had double diagnoses of ADHD and autism spectrum disorder.

We performed a permutation test by randomly labeling 10,000 case-control series within our dataset. Subsequently, we calculated the corresponding CIFs for each permutation by using the hybrid model, and we used right-tailed Mann-Whitney U tests to determine whether the CIF for the *KDM3B* individuals was significantly higher than expected based on random chance. By using this approach, we were able to demonstrate that there is a significant similarity between the faces of individuals with a germline variant

in *KDM3B* when compared to the general ID population (CIF = 2.5962; $p = 0.0054$; Figure 3). This strongly suggests that the individuals with a variant in *KDM3B* have a facial gestalt, and that the computational analysis of facial dysmorphisms can be used to delineate this genetic entity. In the future, when combined with other phenotypic and genetic information, this hybrid facial recognition model might be useful for classifying individuals with variants of unknown significance (VUSs) in *KDM3B*.

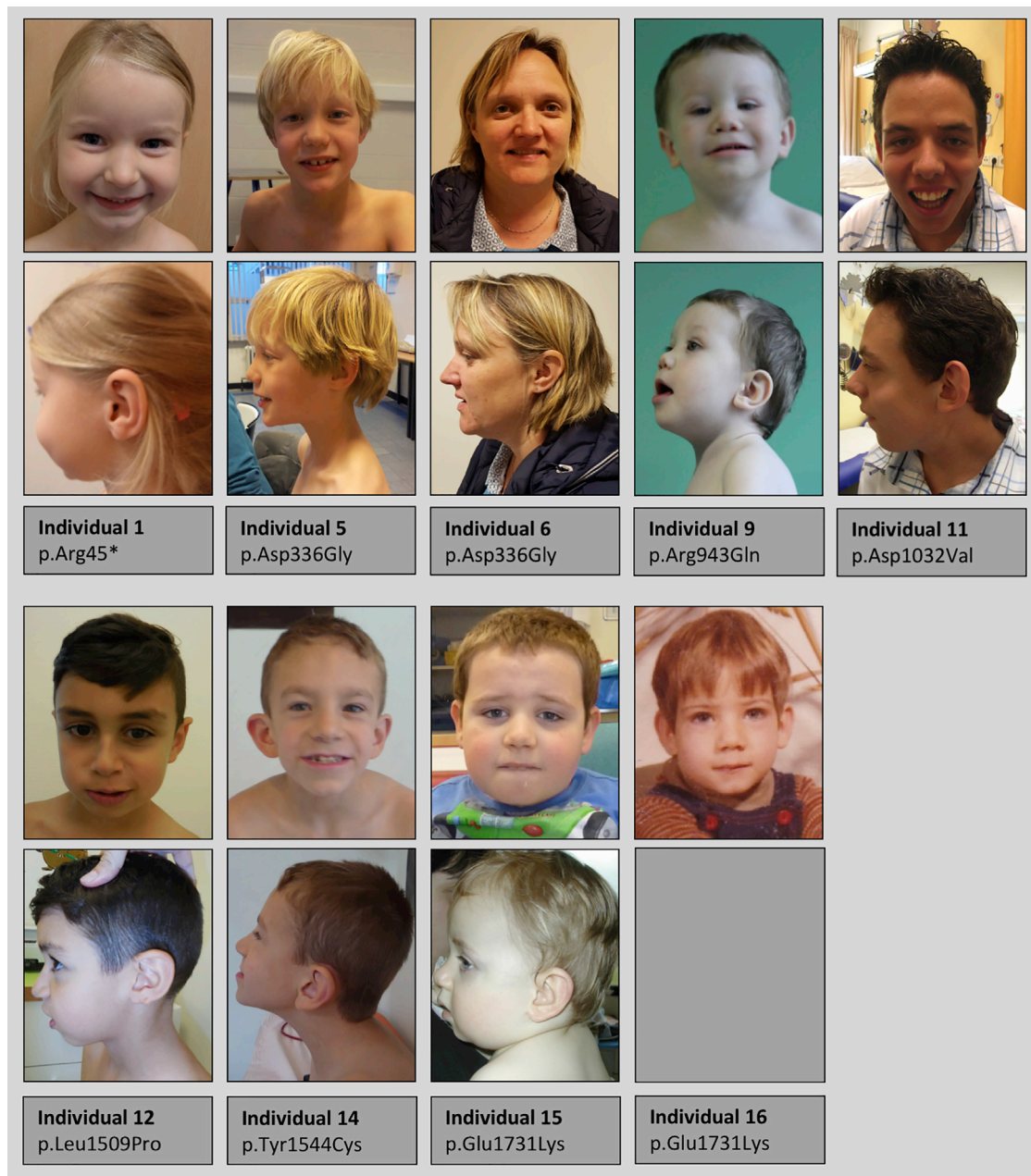


Figure 2. Facial Characteristics of Individuals Carrying Germline Variants in *KDM3B*

Presented are frontal and lateral photographs of 10 of the 17 individuals with a variant in *KDM3B*. Shared facial characteristics include long ears, a prominent nasal tip, a low columella, a thin upper lip, a broad mouth, and a prominent chin.

KDM3B is part of an important group comprising the histone lysine methylases (*KMTs*) and histone lysine demethylases (*KDMs*). This group of proteins is involved in gene regulation and expression.²³ Several of these genes have already been associated with NDDs; for example, *KMT2D* (MIM: 602113) is associated with Kabuki syndrome 1 (MIM: 147920²⁴), and *KDM6A* (MIM: 300128) is associated with Kabuki syndrome 2 (MIM: 300867²⁵). In addition, germline variants in the H3K9 demethylase *JMJD1C* (MIM: 604503), which is a gene that shows large regions of homology with *KDM3B*, are found in individuals with intracranial germ cell tumors and with

NDDs.^{26,27} Rare *de novo* *KDM3B* variants (c.4216C>T [p.Arg1406Trp]²⁸ and c.2624del [p.Leu875Argfs*8])⁴ have been reported in two individuals with schizophrenia and ID, respectively. However, the associated phenotypes have not been fully reported, nor was the causality of these variants confirmed. None of the individuals presented in this study showed signs of schizophrenia.

Faundes et al. recently published an overview of all *KMTs* and *KDMs* associated with disease, and they showed that in these genes, variants resulting in developmental disorders mostly exert their effect through haploinsufficiency.²³ We identified nonsense variants in five

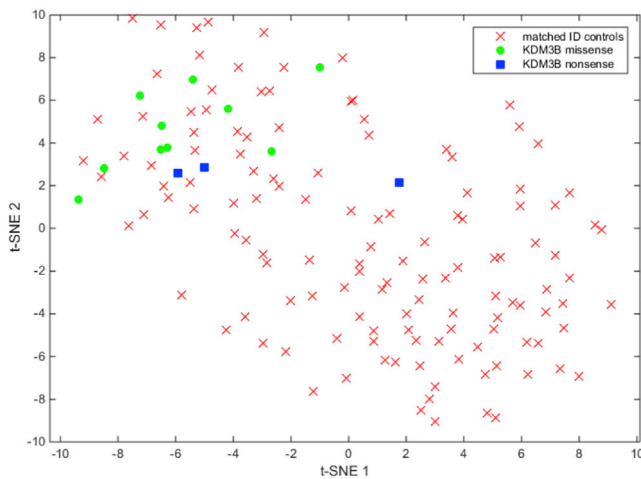


Figure 3. t-SNE Plots Showing the Distribution of 13 Individuals with a Germline Variant in *KDM3B* Versus Controls with Intellectual Disability

t-distributed stochastic neighbor embeddings (t-SNE) plots visualize the distribution of the hybrid feature vectors for both individuals and controls. Relative clustering of individuals with a germline variant in *KDM3B* suggests that this group of individuals with intellectual disability (ID) shows more similarity in facial features than is expected by chance. The control group is matched with the *KDM3B*-mutated group for gender, ethnicity, and age.

individuals (Table 1), implying that haploinsufficiency is the most likely mechanism of disease in our individuals as well. Furthermore, in this paper by Faundes et al., *KDM3B* is among the genes suggested as candidate genes for NDDs on the basis of the high probability of loss-of-function intolerance (pLI) score of 1.00 in the ExAC database. Additionally, in ExAC a Z score of 4.99 was reported, demonstrating a selection against missense variants.

Besides these five individuals with nonsense variants, there were 12 individuals who carried missense variants in *KDM3B*. Notably, two individuals carried missense variants affecting the same amino-acid; these variants were c.2827C>T (p.Arg943Trp) in individual 8 and c.2828G>A (p.Arg943Gln) in individual 9. All missense variants affect residues that are evolutionarily highly conserved across other species (Table 1). To further determine the effect of the missense variants identified, we used the MetaDome web server to generate a tolerance landscape of *KDM3B* (Figure 1B).³⁰ This server uses the gnomAD database to calculate a missense-over-synonymous ratio as a sliding window over the protein. This ratio is then expressed as a tolerance landscape. Herewith, we showed that the Arg943, Leu1509, Glu1731, and Leu1734 variants are located in regions intolerant for missense variation, and the regions surrounding the amino acids Asp1028, Asp1032, and Tyr1544 are highly intolerant regions for missense variation (Table 1). The localization of these variants in intolerant and highly intolerant regions of the gene contributes to the evidence that these variants are pathogenic; it has been described before that variants in gene regions that are depleted of missense variation

are more likely to underlie disease.³¹ According to the MetaDome tolerance landscape, the regions where the Trp117 and Asp336 variants are localized are neutral and tolerant, respectively, meaning that missense variation in these regions is less rare. However, the facial recognition software showed that the faces of the individuals with these two variants do show significant similarity with those of the other individuals. We consider the Trp117 and Asp336 variants as VUSs that require further study.

Additionally, we show that the mutated amino acids in the affected individuals are conserved across the other *KDM3* family members, *KDM3A* (MIM: 611512) and *JMD1C* (Figure 1C); this conservation highlights the potential importance of these specific amino acids. Moreover, the variants clustered within or near two functional domains: the zinc-finger and Jumonji-C domains (Figures 1A and 1C).²⁹ The Jumonji-C domain in *KDM3B* is responsible for the demethylation of histone 3 lysine 9 (H3K9), and it is a highly conserved domain that has ~64% overall amino acid similarity among *KDM3* sub-family members.^{29,32,33}

Furthermore, because *KDM3B* is involved in the demethylation of H3K9, we assessed the mono- and tri-methylation status of H3K9 in HEK293 cells that were overexpressing wild-type and missense mutants of *KDM3B*, but these experiments were inconclusive due to large variability in expression levels (data not shown). Therefore, the functional impact of the missense variants identified remains to be clarified.

This disorder caused by germline variants in *KDM3B* appears to be characterized by a variable clinical presentation. Short stature (<-2.5 SD) was observed in eight individuals (50.0%). Remarkably, *kdm3b*-knockout mice present with a somatic growth restriction, possibly explained by decreased concentrations of insulin-like growth factor-1 (IGF1).³⁴ As low IGF1 levels can be indicative of growth-hormone deficiency, this might be an explanation for the short stature observed in the individuals with a variant in *KDM3B*. IGF1 levels and growth hormone status were not routinely tested in the individuals described in this paper, but one child (individual 13) was found to have isolated growth-hormone deficiency. Also, it is hypothesized by Faundes et al.²³ that variants in genes promoting transcriptional activity appear to cause growth retardation, whereas overgrowth results from variants in transcriptional repressors such as *NSD1* (MIM: 606681) and *EZH2* (MIM: 601573). Because methylation of H3K9 is generally considered to be a repressive mark, demethylation of H3K9 by *KDM3B* is predicted to result in the activation of transcription and thus might explain subsequent growth retardation. Another feature shown by *kdm3b*-knockout mice is subfertility in male mice.³⁵ In accordance, oligospermia was diagnosed in individual 16.

Two individuals were diagnosed with childhood cancer: acute myeloid leukemia at age 13 in individual 2 and Hodgkin lymphoma at age 17 in individual 11. In individual 2, we excluded loss-of-heterozygosity (LOH) of the

germline variant and the possibility of a second hit variant in *KDM3B*. These individuals have been described previously in a study focusing on genetic predisposition for childhood cancer. In this study, we performed exome sequencing on children with cancer and additional features pointing toward genetic predisposition.³⁶ Interestingly, many syndromes, such as Weaver syndrome (MIM: 277590),^{37,38} Rubinstein Taybi syndrome (MIM: 180849),^{39,40} and Sotos syndrome (MIM: 117550),^{41,42} caused by variants in other chromatin-remodeling genes have been described to cause both ID and a mildly increased risk of cancer. Because only two out of 17 individuals in our cohort developed cancer, and both were recruited through a childhood cancer predisposition study³⁶ (introducing an ascertainment bias), it is unclear whether the variants in *KDM3B* are causative of the cancer in these children. However, there are several clues linking variants in *KDM3B* to cancer predisposition. For example, somatic variants in *KDM3B* have been described in different cancer types,^{43,44} and several studies link *KDM3B* alterations to defects and malignancies in the hematopoietic system.^{32,45–47} Particularly interesting is the fact that *kdm3b*-knockout mice show defects in the hematopoietic system, consistent with myelodysplastic syndrome.⁴⁸ Together, these facts suggest that *KDM3B* might play a role in the development of hematopoietic malignancies. However, the assessment of larger cohorts of *KDM3B*-mutated individuals is required to establish whether the incidence of (hematologic) malignancies is indeed enriched in these individuals. On the basis of the current findings, we would not advise screening for malignancies, although vigilance is warranted.

In conclusion, by using exome sequencing we identified 17 individuals with germline, pathogenic variants in *KDM3B*. We show that both *de novo* and inherited variants in *KDM3B* cause a syndrome hallmarked by DD or mild to moderate ID, short stature, and feeding difficulties in infancy. By performing analysis of photographs of the affected individuals with a hybrid facial recognition model, we showed that individuals with a variant in *KDM3B* significantly cluster within a group of ID-affected individuals and thus show a facial gestalt. This model can be used in the future to delineate genetic entities and determine the pathogenicity of VUSs.

Supplemental Data

Supplemental Data can be found online at <https://doi.org/10.1016/j.ajhg.2019.02.023>.

Acknowledgments

I.J.D. was funded by the KiKa Foundation (project number 127). V.H. is funded by the National Institutes of Health (NIH) NICHD R01 HD078592. E.W. was funded by the Dutch Cancer Society (KUN2012-5366). B.C. is a senior clinical investigator of the Fund for Scientific Research, Flanders. This work was partly supported by a research grant from the Research Foundation, Flan-

ders: G028415N to B.C.. We thank Carol Saunders and Laura Cross for their contributions.

Declaration of interests

The authors declare no competing interests.

Received: December 19, 2018

Accepted: February 21, 2019

Published: March 28, 2019

Web Resources

Clinical Face Phenotype Space, https://github.com/ChristofferNellaker/Clinical_Face_Phenotype_Space_Pipeline
ExAC Browser, v.0.3.1., <http://exac.broadinstitute.org>
GenBank, <https://www.ncbi.nlm.nih.gov/genbank/>
GeneMatcher, <https://genematcher.org>
gnomAD Browser, v.r2.0.2., <https://gnomad.broadinstitute.org>
MetaDome, <https://stuart.radboudumc.nl/metadome/>
OMIM, <http://www.omim.org>
OpenFace, <https://cmusatyalab.github.io/openface/>

References

1. Maulik, P.K., Mascarenhas, M.N., Mathers, C.D., Dua, T., and Saxena, S. (2011). Prevalence of intellectual disability: A meta-analysis of population-based studies. *Res. Dev. Disabil.* **32**, 419–436.
2. Ropers, H.H. (2010). Genetics of early onset cognitive impairment. *Annu. Rev. Genomics Hum. Genet.* **11**, 161–187.
3. Deciphering Developmental Disorders, S.; and Deciphering Developmental Disorders Study (2015). Large-scale discovery of novel genetic causes of developmental disorders. *Nature* **519**, 223–228.
4. Deciphering Developmental Disorders, S.; and Deciphering Developmental Disorders Study (2017). Prevalence and architecture of *de novo* mutations in developmental disorders. *Nature* **542**, 433–438.
5. de Ligt, J., Willemsen, M.H., van Bon, B.W., Kleefstra, T., Yntema, H.G., Kroes, T., Vulto-van Silfhout, A.T., Koolen, D.A., de Vries, P., Gilissen, C., et al. (2012). Diagnostic exome sequencing in persons with severe intellectual disability. *N. Engl. J. Med.* **367**, 1921–1929.
6. Vissers, L.E., de Ligt, J., Gilissen, C., Janssen, I., Stehouwer, M., de Vries, P., van Lier, B., Arts, P., Wieskamp, N., del Rosario, M., et al. (2010). A *de novo* paradigm for mental retardation. *Nat. Genet.* **42**, 1109–1112.
7. de Bruin, C., Mericq, V., Andrew, S.F., van Duyvenvoorde, H.A., Verkaik, N.S., Losekoot, M., Porollo, A., Garcia, H., Kuang, Y., Hanson, D., et al. (2015). An *XRCC4* splice mutation associated with severe short stature, gonadal failure, and early-onset metabolic syndrome. *J. Clin. Endocrinol. Metab.* **100**, E789–E798.
8. Rauch, A., Wiczorek, D., Graf, E., Wieland, T., Endeley, S., Schwarzmayr, T., Albrecht, B., Bartholdi, D., Beygo, J., Di Donato, N., et al. (2012). Range of genetic mutations associated with severe non-syndromic sporadic intellectual disability: An exome sequencing study. *Lancet* **380**, 1674–1682.
9. Thiffault, I., Cadioux-Dion, M., Farrow, E., Caylor, R., Miller, N., Soden, S., and Saunders, C. (2018). On the verge of

- diagnosis: Detection, reporting, and investigation of de novo variants in novel genes identified by clinical sequencing. *Hum. Mutat.* 39, 1505–1516.
10. Soden, S.E., Saunders, C.J., Willig, L.K., Farrow, E.G., Smith, L.D., Petrikin, J.E., LePichon, J.B., Miller, N.A., Thiffault, I., Dinwiddie, D.L., et al. (2014). Effectiveness of exome and genome sequencing guided by acuity of illness for diagnosis of neurodevelopmental disorders. *Sci. Transl. Med.* 6, 265ra168.
 11. Sobreira, N., Schiettecatte, F., Valle, D., and Hamosh, A. (2015). GeneMatcher: A matching tool for connecting investigators with an interest in the same gene. *Hum. Mutat.* 36, 928–930.
 12. Lek, M., Karczewski, K.J., Minikel, E.V., Samocha, K.E., Banks, E., Fennell, T., O'Donnell-Luria, A.H., Ware, J.S., Hill, A.J., Cummings, B.B., et al.; Exome Aggregation Consortium (2016). Analysis of protein-coding genetic variation in 60,706 humans. *Nature* 536, 285–291.
 13. Adzhubei, I.A., Schmidt, S., Peshkin, L., Ramensky, V.E., Gerasimova, A., Bork, P., Kondrashov, A.S., and Sunyaev, S.R. (2010). A method and server for predicting damaging missense mutations. *Nat. Methods* 7, 248–249.
 14. Kircher, M., Witten, D.M., Jain, P., O'Roak, B.J., Cooper, G.M., and Shendure, J. (2014). A general framework for estimating the relative pathogenicity of human genetic variants. *Nat. Genet.* 46, 310–315.
 15. Kumar, P., Henikoff, S., and Ng, P.C. (2009). Predicting the effects of coding non-synonymous variants on protein function using the SIFT algorithm. *Nat. Protoc.* 4, 1073–1081.
 16. Boehringer, S., Guenther, M., Sinigerova, S., Wurtz, R.P., Horsthemke, B., and Wieczorek, D. (2011). Automated syndrome detection in a set of clinical facial photographs. *Am. J. Med. Genet. A.* 155A, 2161–2169.
 17. Dudding-Byth, T., Baxter, A., Holliday, E.G., Hackett, A., O'Donnell, S., White, S.M., Attia, J., Brunner, H., de Vries, B., Koolen, D., et al. (2017). Computer face-matching technology using two-dimensional photographs accurately matches the facial gestalt of unrelated individuals with the same syndromic form of intellectual disability. *BMC Biotechnol.* 17, 90.
 18. Hammond, P., Hutton, T.J., Allanson, J.E., Buxton, B., Campbell, L.E., Clayton-Smith, J., Donnai, D., Karmiloff-Smith, A., Metcalfe, K., Murphy, K.C., et al. (2005). Discriminating power of localized three-dimensional facial morphology. *Am. J. Hum. Genet.* 77, 999–1010.
 19. Boehringer, S., Vollmar, T., Tasse, C., Wurtz, R.P., Gillissen-Kaesbach, G., Horsthemke, B., and Wieczorek, D. (2006). Syndrome identification based on 2D analysis software. *Eur. J. Hum. Genet.* 14, 1082–1089.
 20. van der Donk, R., Jansen, S., Schuurs-Hoeijmakers, J.H.M., Koolen, D.A., Goltstein, L., Hoischen, A., Brunner, H.G., Kemmeren, P., Nellaker, C., Vissers, L., et al. (2018). Next-generation phenotyping using computer vision algorithms in rare genomic neurodevelopmental disorders. *Genet. Med.*
 21. Ferry, Q., Steinberg, J., Webber, C., FitzPatrick, D.R., Ponting, C.P., Zisserman, A., and Nellåker, C. (2014). Diagnostically relevant facial gestalt information from ordinary photos. *eLife* 3, e02020.
 22. Amos, B., Ludwiczuk, B., and Satyanarayanan, M. (2016). Openface: A general-purpose face recognition library with mobile applications (CMU School of Computer Science).
 23. Faundes, V., Newman, W.G., Bernardini, L., Canham, N., Clayton-Smith, J., Dallapiccola, B., Davies, S.J., Demos, M.K., Goldman, A., Gill, H., et al. (2018). Histone lysine methylases and demethylases in the landscape of human developmental disorders. *Am. J. Hum. Genet.* 102, 175–187.
 24. Ng, S.B., Bigham, A.W., Buckingham, K.J., Hannibal, M.C., McMillin, M.J., Gildersleeve, H.I., Beck, A.E., Tabor, H.K., Cooper, G.M., Mefford, H.C., et al. (2010). Exome sequencing identifies MLL2 mutations as a cause of Kabuki syndrome. *Nat. Genet.* 42, 790–793.
 25. Lederer, D., Grisart, B., Digilio, M.C., Benoit, V., Crespin, M., Ghariani, S.C., Maystadt, I., Dallapiccola, B., and Verellen-Dumoulin, C. (2012). Deletion of KDM6A, a histone demethylase interacting with MLL2, in three patients with Kabuki syndrome. *Am. J. Hum. Genet.* 90, 119–124.
 26. Saez, M.A., Fernandez-Rodriguez, J., Moutinho, C., Sanchez-Mut, J.V., Gomez, A., Vidal, E., Petazzi, P., Szczesna, K., Lopez-Serra, P., Lucariello, M., et al. (2016). Mutations in JMJD1C are involved in Rett syndrome and intellectual disability. *Genet. Med.* 18, 378–385.
 27. Wang, L., Yamaguchi, S., Burstein, M.D., Terashima, K., Chang, K., Ng, H.K., Nakamura, H., He, Z., Doddapaneni, H., Lewis, L., et al. (2014). Novel somatic and germline mutations in intracranial germ cell tumours. *Nature* 511, 241–245.
 28. Guipponi, M., Santoni, F.A., Setola, V., Gehrig, C., Rotharmel, M., Cuenca, M., Guillin, O., Dikeos, D., Georgantopoulos, G., Papadimitriou, G., et al. (2014). Exome sequencing in 53 sporadic cases of schizophrenia identifies 18 putative candidate genes. *PLoS ONE* 9, e112745.
 29. Brauchle, M., Yao, Z., Arora, R., Thigale, S., Clay, I., Inverardi, B., Fletcher, J., Taslimi, P., Acker, M.G., Gerrits, B., et al. (2013). Protein complex interactor analysis and differential activity of KDM3 subfamily members towards H3K9 methylation. *PLoS ONE* 8, e60549.
 30. Wiel, L., Baakman, C., Gilissen, D., Veltman, J.A., Vriend, G., and Gilissen, C. (2019). MetaDome: Pathogenicity analysis of genetic variants through aggregation of homologous human protein domains. *bioRxiv*. <https://doi.org/10.1101/509935>.
 31. Ge, X., Gong, H., Dumas, K., Litwin, J., Phillips, J.J., Waisfisz, Q., Weiss, M.M., Hendriks, Y., Stuurman, K.E., Nelson, S.F., et al. (2016). Missense-depleted regions in population exomes implicate ras superfamily nucleotide-binding protein alteration in patients with brain malformation. *NPJ Genom. Med.* 1.
 32. Kim, J.Y., Kim, K.B., Eom, G.H., Choe, N., Kee, H.J., Son, H.J., Oh, S.T., Kim, D.W., Pak, J.H., Baek, H.J., et al. (2012). KDM3B is the H3K9 demethylase involved in transcriptional activation of *lmo2* in leukemia. *Mol. Cell. Biol.* 32, 2917–2933.
 33. Kim, S.M., Kim, J.Y., Choe, N.W., Cho, I.H., Kim, J.R., Kim, D.W., Seol, J.E., Lee, S.E., Kook, H., Nam, K.I., et al. (2010). Regulation of mouse steroidogenesis by WHISTLE and JMJD1C through histone methylation balance. *Nucleic Acids Res.* 38, 6389–6403.
 34. Liu, Z., Chen, X., Zhou, S., Liao, L., Jiang, R., and Xu, J. (2015). The histone H3K9 demethylase *Kdm3b* is required for somatic growth and female reproductive function. *Int. J. Biol. Sci.* 11, 494–507.
 35. Liu, Z., Oyola, M.G., Zhou, S., Chen, X., Liao, L., Tien, J.C., Mani, S.K., and Xu, J. (2015). Knockout of the histone demethylase *Kdm3b* decreases spermatogenesis and impairs male sexual behaviors. *Int. J. Biol. Sci.* 11, 1447–1457.

36. Diets, I.J., Waanders, E., Ligtenberg, M.J., van Bladel, D.A.G., Kamping, E.J., Hoogerbrugge, P.M., Hopman, S., Olderode-Berends, M.J., Gerkes, E.H., Koolen, D.A., et al. (2018). High yield of pathogenic germline mutations causative or likely causative of the cancer phenotype in selected children with cancer. *Clin. Cancer Res.* *24*, 1594–1603.
37. Tatton-Brown, K., Murray, A., Hanks, S., Douglas, J., Armstrong, R., Banka, S., Bird, L.M., Clericuzio, C.L., Cormier-Daire, V., Cushing, T., et al.; Childhood Overgrowth Consortium (2013). Weaver syndrome and EZH2 mutations: Clarifying the clinical phenotype. *Am. J. Med. Genet. A.* *161A*, 2972–2980.
38. Usemann, J., Ernst, T., Schäfer, V., Lehmborg, K., and Seeger, K. (2016). EZH2 mutation in an adolescent with Weaver syndrome developing acute myeloid leukemia and secondary hemophagocytic lymphohistiocytosis. *Am. J. Med. Genet. A.* *170A*, 1274–1277.
39. Bourdeaut, F., Miquel, C., Richer, W., Grill, J., Zerah, M., Grison, C., Pierron, G., Amiel, J., Krucker, C., Radvanyi, F., et al. (2014). Rubinstein-Taybi syndrome predisposing to non-WNT, non-SHH, group 3 medulloblastoma. *Pediatr. Blood Cancer* *61*, 383–386.
40. de Kort, E., Conneman, N., and Diderich, K. (2014). A case of Rubinstein-Taybi syndrome and congenital neuroblastoma. *Am. J. Med. Genet. A.* *164A*, 1332–1333.
41. Tatton-Brown, K., Douglas, J., Coleman, K., Baujat, G., Cole, T.R., Das, S., Horn, D., Hughes, H.E., Temple, I.K., Faravelli, F., et al.; Childhood Overgrowth Collaboration (2005). Genotype-phenotype associations in Sotos syndrome: an analysis of 266 individuals with NSD1 aberrations. *Am. J. Hum. Genet.* *77*, 193–204.
42. Villani, A., Greer, M.C., Kalish, J.M., Nakagawara, A., Nathanson, K.L., Pajtler, K.W., Pfister, S.M., Walsh, M.F., Wasserman, J.D., Zelley, K., et al. (2017). Recommendations for cancer surveillance in individuals with RASopathies and other rare genetic conditions with increased cancer risk. *Clin. Cancer Res.* *23*, e83–e90.
43. Forbes, S.A., Beare, D., Boutselakis, H., Bamford, S., Bindal, N., Tate, J., Cole, C.G., Ward, S., Dawson, E., Ponting, L., et al. (2017). COSMIC: Somatic cancer genetics at high-resolution. *Nucleic Acids Res.* *45* (D1), D777–D783.
44. Paolicchi, E., Crea, F., Farrar, W.L., Green, J.E., and Danesi, R. (2013). Histone lysine demethylases in breast cancer. *Crit. Rev. Oncol. Hematol.* *86*, 97–103.
45. Xu, X., Nagel, S., Quentmeier, H., Wang, Z., Pommerenke, C., Dirks, W.G., Macleod, R.A.F., Drexler, H.G., and Hu, Z. (2018). KDM3B shows tumor-suppressive activity and transcriptionally regulates HOXA1 through retinoic acid response elements in acute myeloid leukemia. *Leuk. Lymphoma* *59*, 204–213.
46. Hu, Z., Gomes, I., Horrigan, S.K., Kravarusic, J., Mar, B., Arbieva, Z., Chyna, B., Fulton, N., Edassery, S., Raza, A., and Westbrook, C.A. (2001). A novel nuclear protein, 5qNCA (LOC51780) is a candidate for the myeloid leukemia tumor suppressor gene on chromosome 5 band q31. *Oncogene* *20*, 6946–6954.
47. MacKinnon, R.N., Kannourakis, G., Wall, M., and Campbell, L.J. (2011). A cryptic deletion in 5q31.2 provides further evidence for a minimally deleted region in myelodysplastic syndromes. *Cancer Genet.* *204*, 187–194.
48. Li, S., Ali, S., Duan, X., Liu, S., Du, J., Liu, C., Dai, H., Zhou, M., Zhou, L., Yang, L., et al. (2018). JMJD1B demethylates H4R3me2s and H3K9me2 to facilitate gene expression for development of hematopoietic stem and progenitor cells. *Cell Rep.* *23*, 389–403.